WiLay: A Two-Layer Human Localization and Activity Recognition System Using WiFi

2021 IEEE 93rd Vehicular Technology Conference (VTC2021-Spring) | 978-1-7281-8964-2/20/$31.00 ©2021 IEEE | DOI: 10.1109/VTC2021-Spring51267.2021.9448863

Jinyang Huang*†, Bin Liu*†, Hongxing Jin*†, Nenghai Yu*†
*School of Information Science and Technology, University of Science and Technology of China, Hefei, China
†Key Laboratory of Electromagnetic Space Information, Chinese Academy of Science, Hefei, China
{huangjy,jhx0112}@mail.ustc.edu.cn, {flowice,ynh}@ustc.edu.cn

***Abstract*— Human activity monitoring (HAM) in the home environment has become increasingly important due to its broad applications including elder care, and well-being management. Recently, some state-of-the-art WiFi-based HAM systems have been proposed due to its properties of non-intrusive and privacy-friendly. However, their key drawback lies in ignoring the crucial impact of human position on HAM. To solve this problem, we present a two-layer WiFi-based HAM system (WiLay), which combines human activity recognition (HAR) with indoor human location (IHL) to provide more integrated information for HAM. Specifically, in the first layer, WiLay adopts the high-frequency energy (HFE) feature of WiFi signals to detect human moving. Then, in the second layer, different processing methods are employed for processing different types of motions accordingly. When the subject activities are static (SAs, the activity without position change), e.g., standing and sitting, WiLay locates the subject before recognizing the specific motion. On the contrary, when the activities are the moving activities (MAs), to reduce the loss of motion information, WiLay employs a comprehensive classifier generated by all different subcarrier classifiers voting, to recognize these MAs accurately. Extensive experimental results show that WiLay has high accuracy with a 99.9% SA/MA detection accuracy rate in the first layer, and a 99.7% location accuracy rate with 98.1% recognition performance for SAs and 90.2% recognition performance for MAs in the second layer.**

I. Introduction

As a fundamental technology in the field of human activity monitoring (HAM), human activity recognition (HAR) is a well-researched topic and has achieved significant progress in recent years, e.g., smart homes, smart cities, security monitor, and virtual reality games [1]. Various techniques ranging from vision-based to sensor-based solutions have been proposed and well studied [2]–[7]. Vision-based approaches usually equipped with high-resolution video cameras to record the human movement. Accordingly, these records are classified into distinct motions by using deep learning. However, the installed high-resolution cameras for these methods are expensive to implement. Besides, the privacy intrusion and inherent requirement for light conditions limit the large-scale application of this method [8]. Sensor-based HAR systems usually extract sensor information, e.g., acceleration information, and gyro information, to catch the human body movements [5]–[7]. However, it requires subjects to carry wearable sensors all the time, which is usually uncomfortable for people, especially for elders and children.

In recent years, with the rapid deployment of wireless networks, several device-free approaches, e.g., dedicated radio frequency (DRF)-based methods and WiFi-based methods have inspired more and more applications [9]. Their crucial superiorities over camera-based and sensor-based approaches are that they preserve user privacy, do not require lighting, and do not require subjects to carry any wearable sensors. DRF-based HAM systems employ the specialized hardware to measure the Doppler shift in signals reflected by human bodies to classify distinct motions. However, specialized DRF equipment is irreplaceable, and the equipment is extremely expensive.

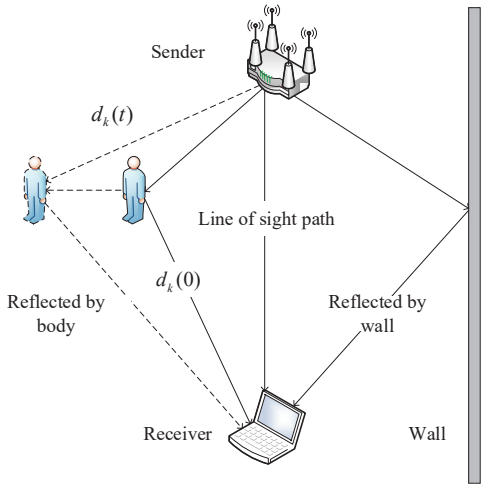

Fig. 1 Signal propagation model with people moving.

Compared with DRF-based HAM methods, WiFi-based methods basically utilize commodity WiFi devices without using other dedicated equipment to collect two different kinds of signals, i.e., *Received Signal Strength Indication* (RSSI) and *Channel State Information* (CSI) [10]. In particular, RSSI as the average measured power of received signals extracted from the MAC layer is a coarse-grained channel measurement. This is because RSSI falls entirely in the amplitude domain, while the phase domain is totally neglected. Compared with RSSI, CSI is a fine-grained measurement derived from the physical layer of WiFi devices and its features are descriptions of motion from different perspectives, i.e., the amplitude domain and the phase domain. Therefore, more information can be obtained from CSI.

Significant progress of WiFi CSI has been made in applications in indoor human location (IHL) [11], [12], motion detection [13], [14], and HAR [15]–[18]. Spotif [11] employed a special AoA estimation and direct path filtering approach to provides accurate indoor location services by using off-the-shelf WiFi. QGesture [18] designed a gesture recognition system that extracted CSI values provided by commodity WiFi devices to measure the movement distance and direction of human hands. However, these methods usually separated IHL and HAR, and only completed one of the tasks, which can not

978-1-7281-8964-2/21/$31.00 ©2021 IEEE

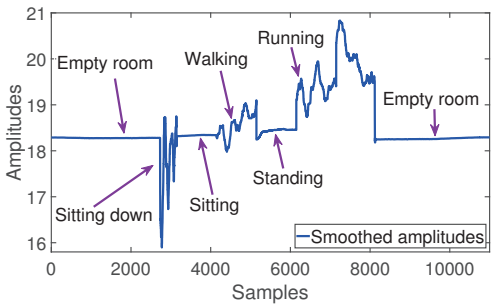

Fig. 2 CSI amplitude series for different activities.

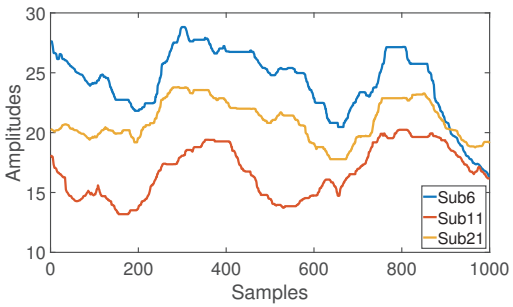

Fig. 3 The CSI amplitude series of different subcarriers for running motion.

provide a satisfactory HAM service. This is because the specific people's status cannot be correctly judged by only recognizing some static activities (the activity without position change, SAs) without position information. For example, the same fall down motion means different in the kitchen and bed.

Therefore, to provide a better HAM service, in this paper, we propose WiLay, a two-layer non-intrusive HAM system that reasonably combines HAR and IHL to provide more integrated motion information. Since the positions of SAs are located at first, Wilay can more accurately determine the user's status in the HAR process. Besides, WiLay leverages cheap and widely deployed WiFi devices, and do not require subjects to carry any sensors. The main contributions of this work are as follows:

1) To the best of our knowledge, we are the first to design a two-layer HAM system to distinguish the motions with or without location information to realize both IHL and HAR. WiLay comprehensively combines moving detection, IHL and HAR functions using WiFi to provide more integrated information for HAM.
2) Since the recognition difficulty level of moving activities (MAs) and SAs are distinct, different signal processing schemes are designed in WiLay for different types of activities (MAs and SAs) to tradeoff the computational complexity of CSI and recognition performance.
3) We prototype WiLay on off-the-shelf WiFi devices and validate its performance in various indoor environments. Extensive experiment results demonstrate that WiLay can distinguish the SAs and MAs reliably, and consistently make a commendable performance compared with other methods, with 99.7% IHL precision rate and 93.7% HAR precision rate on average.

The rest of this paper is organized as follows. Section II introduces the proposed non-invasive IHL and HAM system WiLay in detail. Then, the experiments and extensive evaluation of WiLay are described in Section III. Finally, Section IV concludes the overall work.

II. The WiLay System

A. Channel State Information

According to the IEEE 802.11n standard [19], the network interface controllers (NICs) can monitor the wireless channel continuously using CSI which describes channel response and can be extracted at the receiver. Moreover, both the amplitude and the phase information of each subcarrier are depicted in CSI. Due to the fact that WiFi basically employs *Orthogonal Frequency Division Multiplexing* (OFDM) technology, the channel between each antenna consists of multiple subcarriers.

Let $\boldsymbol{X}_i$ and $\boldsymbol{Y}_i$ donate the transmitted and the received signal vectors of the i^{th} transmitter-receiver pair, respectively. Therefore, the two signal vectors can be modeled as [20]:

$$\boldsymbol{Y}_i = \boldsymbol{H}_i \boldsymbol{X}_i + \boldsymbol{n} \tag{1}$$

where $\boldsymbol{H}_i$ is the channel matrix of the i^{th} transmitter-receiver pair and $\boldsymbol{n}$ is the additive noise vector. $\boldsymbol{H}$ in the above formula can be estimated at the receiver when a known sequence of $\boldsymbol{X}_i$ is transmitted. Besides, the estimated $\boldsymbol{H}_i$ for N subcarriers can be expressed as:

$$\boldsymbol{H} = [\boldsymbol{h}_1, \boldsymbol{h}_2, ..., \boldsymbol{h}_i, ..., \boldsymbol{h}_N]^T \tag{2}$$

Here, the frequency response of k^{th} subcarrier can be represented:

$$\boldsymbol{h}_k = |\boldsymbol{h}_k| \, e^{j \sin \theta_k}, \tag{3}$$

where $|\boldsymbol{h}_k|$ and θ_k are the amplitude and the phase of subcarrier k, respectively. Using an Intel 5300 NIC with 3 antennas and the router with two antennas, WiLay can receive 6 CSI streams simultaneously. Besides, the CSIs in Wilay are extracted by CSITOOL [21], which collects 30 subcarrier data in one stream. Therefore, 180 ($3 \times 2 \times 30$) groups of CSI values are extracted from each packet, and the value of $\boldsymbol{H}$ can be expressed as:

$$\boldsymbol{H}_{i,j} = \begin{bmatrix} \boldsymbol{h}_{1,1} & \boldsymbol{h}_{1,2} & \boldsymbol{h}_{1,3} & \dots & \boldsymbol{h}_{1,30} \\ \boldsymbol{h}_{2,1} & \boldsymbol{h}_{2,2} & \boldsymbol{h}_{2,3} & \dots & \boldsymbol{h}_{2,30} \\ \vdots & \vdots & \vdots & \ddots & \vdots \\ \boldsymbol{h}_{6,1} & \boldsymbol{h}_{6,2} & \boldsymbol{h}_{6,3} & \dots & \boldsymbol{h}_{6,30} \end{bmatrix}, \tag{4}$$

where $\boldsymbol{h}_{i,k}$ is the CSI value for k^{th} subcarrier in i^{th} stream.

B. Radio Propagation Model

The crucial principle of WiFi CSI can be used to capture human movement and record the human location is that the motion and the location of the subject affect the wireless propagation paths. As shown in Fig.1, in a typical indoor environment, due to the surroundings such as walls and human bodies, there is one main path (Line-Of-Sight, LOS) and several reflected paths (None-Line-Of-Sight, NLOS), which is known as *Multipath Propagation*. According to the free space model, the changes in a path length lead to the changes in the amplitude and the phase of the WiFi CSIs on the corresponding path. Furthermore, subjects locate in different places or perform distinct motions cause different changes in CSIs. Therefore, the movement and location can be determined accordingly by suitable processing.

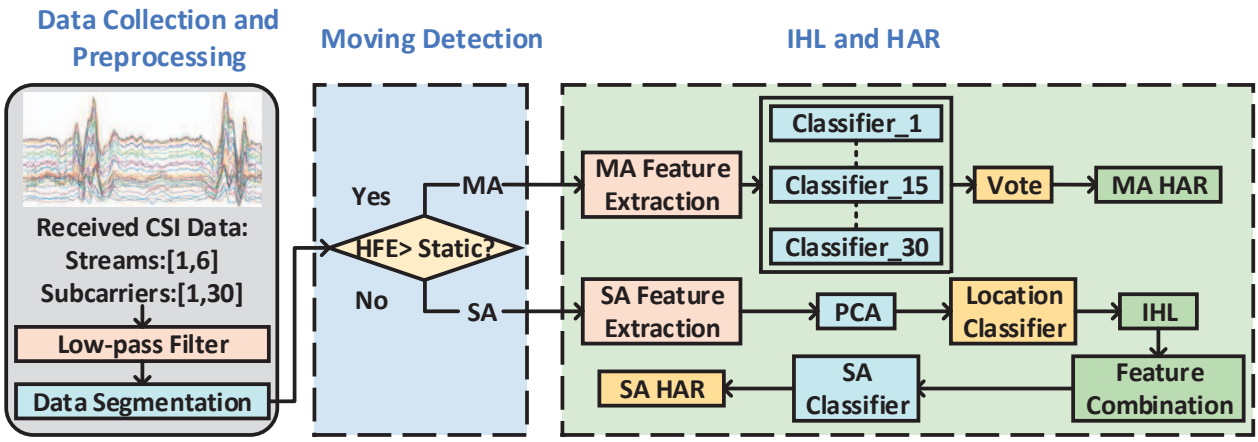

Fig. 4 Flow diagram of WiLay.

Fig. 2 shows the amplitude changes for different motions. The amplitude of CSI is a straight line with little variation when there are no people in the room. However, the fluctuations become significant when people are moving. Therefore, people moving can be detected by the varying level of the CSI amplitude. Fig. 3 depicts the different subcarrier amplitudes in one stream for running motion samples, which means that the same activity similarly affects different subcarriers. Moreover, the closer frequencies of the subcarriers, the correlation between these subcarriers is stronger. Thus, an effective subcarrier fusion method is needed to reduce computational complexity and maintain motion information.

C. System Overview

WiLay is a non-invasive HAM system, which reasonably combines IHL and HAR to provide a more complete subject behavior information, without adding extra hardware or wearable sensors. The workflow of the WiLay system is shown in Fig.4, which contains three main parts, i.e., Data collection, Moving detection, and IHL and HAR. In the first part, WiLay takes the time-series of CSI amplitude from off-the-shelf WiFi hardware as input. Then, the *Moving average filter* is adopted to filter out the noise to obtain reliable CSI time series. Next, in the second part, *Discrete Wavelet Transform* (DWT) method [22] is employed to calculate the high-frequency energy (HFE) of CSI, which is used to distinguish whether the human is moving or not. Finally, in the third part, when human motion is SA, WiLay compares position characteristics with the presupposed configuration to accomplish IHL before classifying the specific activity. However, when the newly detected moving target (MAs) is verified, the subject motion will be recognized directly. It's worth mentioning that, different subcarrier fusion methods are used for distinct type motions to better tradeoff the computational complexity and the performance.

D. CSI Data Extraction and Segmentation

The CSI values are inherently noisy due to the frequent changes in the internal CSI reference levels and the external environment changes, e.g., temperature and humidity. Thus, the *moving average filter* (the sliding window size is 20 samples) is employed in WiLay system to reduce noises since this filter can effectively remove noises with high speed and low computational complexity. Then, every five second CSI time-series are segmented into one activity sample.

E. Activity Detection

To employ different subcarrier fusion methods for distinct types of activities to tradeoff the computational complexity and the accuracy, the subject moving (judging the motion is SA or MA) should be detected at first. Specifically, the HFE of CSI is used to detect human moving. To obtain HFE, the DWT coefficients should be calculated, which can be expressed:

$$C[l] = \sum_{t=0}^{l-1} d[2l-t]\, g[t] \tag{5}$$

$$D[l] = \sum_{t=0}^{l-1} d[2l-t]\, h[t] \tag{6}$$

where $d[l]$ is the CSI amplitude series and its length is l. $C[l]$ and $D[l]$ are the approximation coefficient and the detail coefficient, and represent the low-frequency part and the high-frequency part of $d[l]$, respectively. Besides, $g[l]$ and $q[l]$ are the low pass filter and the high pass filter(db1 wavelet basis), respectively. Thus, the HFE can be calculated as Eq.(7):

$$HFE = \sum_{t=1}^{l} (D[t])^2 \tag{7}$$

Then, a suitable classification algorithm is used to judge the motion types based on the observations in Fig. 2(a), when the motion is SA, the CSI amplitudes stay a low level and cause a small HFE due to the stable propagation paths, and when the motion becomes MAs, the CSI amplitudes rise rapidly and cause a big HFE since the fast-changing propagation paths. Specifically, the HFE of 30 subcarriers in one motion sample is used to constitute a multidimensional vector as the input firstly. Then, the Euclidean distance is employed to calculate the distances between this testing sample vector and the training sample vectors. Finally, the testing sample type is determined as the training sample type with the shortest distance.

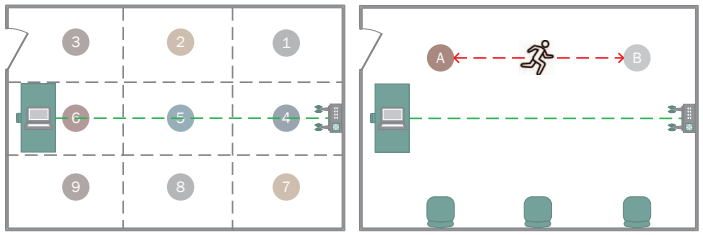

(a) IHL for SAs: the static participant in different locations. **(b)** HAR for MAs: the moving people running between A and B.

Fig. 5 The illustration of IHL and HAR scenes.

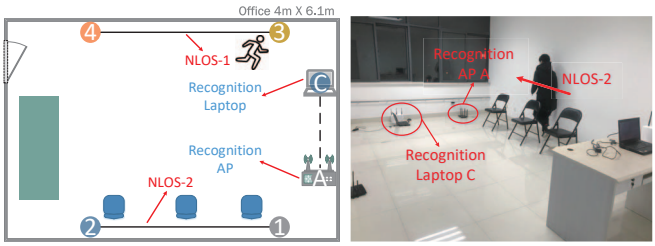

(a) The schematic diagram. **(b)** Experimental setting.

Fig. 6 The location diagram of different NLOS paths.

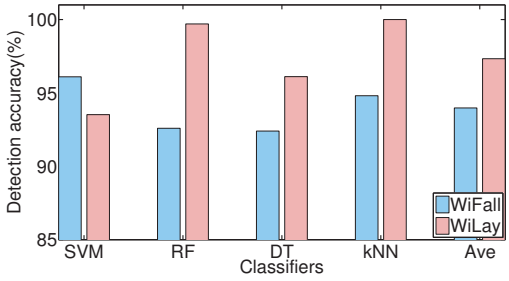

Fig. 7 Moving detection accuracy.

F. IHL and HAR

The motion detection result determines the tasks which WiLay executes in this part. For moving subjects, WiLay only recognizes its activities without locating. However, since the location information is crucial for SAs, WiLay locates the human position at first and then recognizes its specific motion.

1) HAR for MAs: As mentioned in Section II-B, human movement leads to changing amplitudes of CSI, WiLay first calculates the motion-related CSI amplitude features, i.e., variance, the variance of variances(VOV), information entropy, and frequency domain maximum value to maximize the difference between distinct motions. Specifically, the above three features need to be explained clearly. The VOV is calculated as follows. Firstly, we segment the CSI series of one motion sample into m sub-groups, and then we calculate the variance of each sub-groups to compose a new sequence. Next, the variance of the new sequence is the VOV, which can be expressed as:

$$\begin{aligned} \mu\left(\sigma^2\right) &= \tfrac{1}{m}\sum_{t=1}^{m}{\sigma^2}_t \\ VOV &= \tfrac{1}{m}\sum_{t=1}^{m}\left({\sigma^2}_t - \mu\left(\sigma^2\right)\right)^2 \end{aligned} \tag{8}$$

where m is the number of sub-groups (25 in our case), and ${\sigma_t}^2$ denotes the variance of the t^{th} sub-group. μ represents the mean of the new sequence. Thus, the variance of the new sequence VOV is obtained. Besides, the information entropy means the frequency domain entropy, and the frequency domain maximum is the maximum value of the frequency domain sequence calculated by *Fast Fourier Transformation*.

After the features are extracted, WiLay first builds one classifier for each subcarrier and then obtains the final MA classification result by the voting of these classifier recognition results. Specifically, each subcarrier features are classified separately by each classifier at first. Then, according to the principle of *minority subordinating to the majority*, the most classified motion result in all subcarrier classifiers is chosen as the final recognized motion. This is because that the rapidly changing CSI waveforms (when the motion is MAs) contain more motion information than the slowly changing CSI waveforms (when the motion is SAs), and the voting approach is a more efficient way to integrate the motion information of all subcarriers. Thus, the MA motion information can be maintained at a maximum level.

2) IHL and HAR for SAs: The fundamental of IHL is that human in different places leads to distinct multipath propagation. Thus, effective CSI propagation features are useful to classify different locations. In particular, WiLay extracts the position-related CSI features, i.e., mean, maximum, minimum, median, upper and lower quartile values at First. Next, unlike the MA processing part, PCA [23] is employed to fuse the features of different subcarriers to reduce the feature dimension and to maintain the motion information. Then, the location features are classified. After the position is determined, WiLay combines the motion-related features of MA and the location-related features of SA to form the total features. Finally, to recognize the specific SA, the total features of each motion are classified.

III. Experiment and Evaluation

A. Experiment Setting

We conduct the experiments in a typical office covering about $4m \times 6m$ area with daily used a table and chairs. To evaluate IHL and HAR performances of WiLay, we first divide the office into nine areas as shown in Fig.5(a) and set a road between points A and B to collect human movements as shown in Fig.5(b). WiLay is implemented on Thinkpad 420i laptop with Intel 5300 NIC and operated in Ubuntu 14.04. The laptop connects to a TP-LINK wireless router (TP-Link WDR7500) and forms a wireless link to collect per sample CSI at a rate of 100 samples per second using CSITOOL [21]. The connected router has two antennas and runs in the 2.4 GHz frequency band with the 20 MHz bandwidth channel. Besides, the NIC is equipped with three antennas. Therefore, the 2×3 system produces six streams and achieves spatial diversity. We conduct WiLay algorithms using MATLAB and Python platform in this prototype.

Since signal refraction caused by NLOS paths affect the signal quality of CSI, the recognition performance of the WiFi-based HAR system is also affected. To evaluate the impact of NLOS paths caused by walls and locations on different WiFi-based HAR systems, as shown in Fig. 6, we change the position of the recognition AP and the recognition laptop and repeat the various motions on two NLOS paths (NLOS-1, NLOS-2) accordingly.

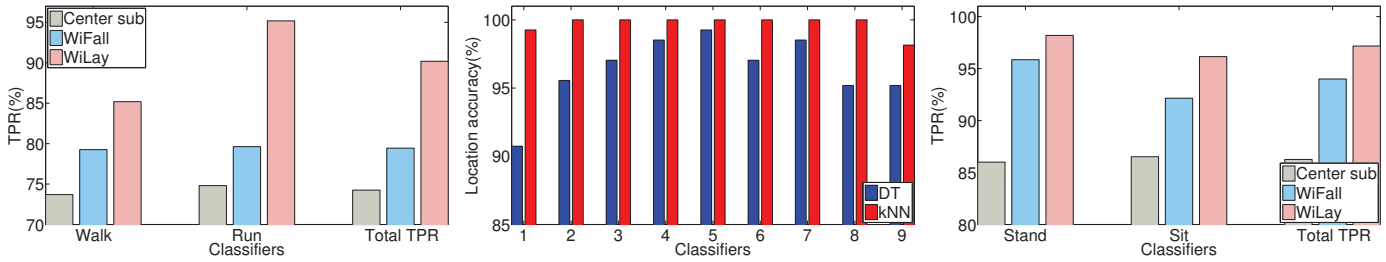

(a) TPRs of different subcarrier algorithms for MAs. **(b)** Location accuracy rates for SAs. **(c)** TPRs of different subcarrier algorithms for SAs.

Fig. 8 The performance of WiLay compared with other methods.

B. Evaluation Metrics

The following metrics are used to evaluate the performance of WiLay.

1) ***Moving Detection Rate (MDR)****:* MDR is defined as the ratio of the number of correctly detected activities $F_{correct}$ to the number of the whole detected activities F_{total}, which evaluates the performance of the moving detection (SA/MA detection accuracy) of WiLay and can be expressed as:

$$MDR = \frac{F_{correct}}{F_{total}} \times 100\% \tag{9}$$

2) ***True Positive Rate (TPR)****:* TPR is defined as the proportion of the number of correctly classified activities in one category $P_{correct}$ to the number of classified activities in this categoryP_{total}, which can be represented as follows:

$$TPR = \frac{P_{correct}}{P_{total}} \times 100\% \tag{10}$$

3) ***Recognition Accuracy Rate (RAR)****:* RAR is defined as the ratio of the number of all correctly classified activities $R_{correct}$ to the number of all classified activities R_{total}, which can be expressed as follows:

$$RAR = \frac{R_{correct}}{R_{total}} \times 100\% \tag{11}$$

C. Performance Evaluation

1) ***Moving Detection Accuracy****:* We first evaluate the feasibility of moving detection in the office. Five different states are tested in the office as shown in Fig.5(a), i.e., Empty rooms, human sitting in position A, human standing in position A, human walking between positions A and B, and human running between position A and B. The first three states are considered as SAs, whereas the last two states are judged as MAs. We perform this experiment on five participants and each participant repeats 54 times for each action and state. Thus, five volunteers totally provide $5\times5\times54$ motion samples. Then, four classical classification algorithms, i.e., Support Vector Machine (SVM), Random Forest (RF), Decision Tree (DT), and *K-Nearest Neighbor* (kNN) are used to detect human moving. A Python module *Scikit-learn* [24] as the machine learning library is adopted to quickly implement these classifiers. Moreover, 10-fold cross-validation is employed to avoid overfitting [25]. In particular, we compare our method with the state-of-the-art method WiFall [26], which used the average CSI of five successive subcarriers algorithm to fuse all CSI subcarrier data.

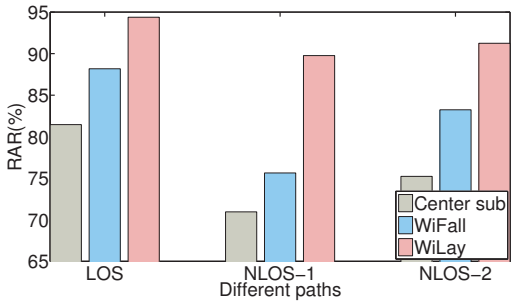

Fig. 9 The performance influenced by the NLOS.

The MDRs are shown in Fig.7, which indicates WiLay has better performance than WiFall in most kinds of classifiers, especially for kNN with the MDR reaching 100%. This clearly shows that Wilay can effectively detect the movement began in an indoor environment.

2) ***HAR Accuracy for MAs****:* As defined above, MAs mean subjects have position changes during the duration of the activity, e.g., walking and running. Here, we test WiLay HAR performance by collecting CSI data when the subject walking and running between positions A and B. Similarly, five participants aggregately provide $5 \times 2 \times 54$ MA samples. Two pioneer baseline subcarrier fusion methods are tested by the same classifier kNN to compare with the MA recognition performance of WiLay, which are choosing the center frequency subcarrier method, and using the average CSI of five successive subcarriers method (WiFall [26]). Fig.8(a) shows the performance of different subcarrier fusion methods for the two MAs, which depicts WiLay has better performance than other methods in all cases. The crucial reason is that the WiLay voting algorithm maintains the motion information of all subcarriers, while others lead to much motion information loss in the process of data dimension reduction.

3) ***IHL and HAR performance for SAs****:* To evaluate the IHL accuracy rate of WiLay, the office is separated into nine areas as shown in Fig.5(a) and each participant repeats 54 times for every SA except empty (standing and sitting) in one area. Therefore, five volunteers totally offer $5 \times 54 \times 2 \times 9$ SA samples. Besides, Fig.8(b) shows the location accuracy rates of WiLay in each area. We can observe that the average accuracy rate of nine areas using DT achieves 96.34%, and the average accuracy rate using kNN achieves 99.71%, which means WiLay has particularly good performance in IHL. After the location is determined, the specific SAs are recognized by the kNN classifier accordingly. Specifically, Fig.8(c) depicts the SA TPRs for the various subcarrier fusion approaches.

We observe that WiLay achieves better performance than other subcarrier fusion methods in all kinds of activities. Moreover, SAs like stand has better recognition performance, whereas sit has lower accuracy. This is possibly due to the relatively larger body motion involvement in standing. Consequently, more details of the target motion could be captured by CSI measurement.

*4) **The Impact of NLOS paths on WiLay Performance**:* Fig. 9 shows the performance of various algorithms under different NLOS path impact. We can observe that NLOS paths downgrade the performance of each algorithm, and the negative effect is more significant for the path (NLOS-1), which is farther away from the recognition AP. Nevertheless, WiLay can always achieve the best performance in all paths. Since more motion information is maintained due to the valid subcarrier voting algorithms, WiLay is more robust to different NLOS paths and positions.

IV. Conclusion

Location information is extremely meaningful for HAR. However, the most existed works separate IHL and HAR and only study one of them in a HAM system. In this paper, we propose WiLay, a two-layer WiFi-based HAM system that reasonably combines IHL and HAR to provide more integrated information for HAM, and leverages the fine-grained information with the commodity WiFi devices. Extensive experiments with different types of motions are implemented in various scenarios, and the results show that WiLay can achieve superior performance on IHL accuracy rates and HAR TPRs over existing approaches. For future works, we want to combine CSI phases and amplitudes to achieve indoor location without pre-segmentation to further enhance the robustness of the system to position changes.

V. Acknowledgment

This work is partially supported by the National Natural Science Foundation of China under grants No. 61202406 and 61371192. We would like to thank the editors and anonymous reviewers for their insightful comments and constructive feedback.

References

[1] O. D. Lara and M. A. Labrador, "A survey on human activity recognition using wearable sensors," *IEEE communications surveys & tutorials*, vol. 15, no. 3, pp. 1192–1209, 2012.

[2] M. Ma, H. Fan, and K. M. Kitani, "Going deeper into first-person activity recognition," in *Proceedings of the IEEE Conference on Computer Vision and Pattern Recognition*, 2016, pp. 1894–1903.

[3] G. Abebe and A. Cavallaro, "A long short-term memory convolutional neural network for first-person vision activity recognition," in *Proceedings of the IEEE International Conference on Computer Vision*, 2017, pp. 1339–1346.

[4] T. Bagautdinov, A. Alahi, F. Fleuret, P. Fua, and S. Savarese, "Social scene understanding: End-to-end multi-person action localization and collective activity recognition," in *Proceedings of the IEEE Conference on Computer Vision and Pattern Recognition*, 2017, pp. 4315–4324.

[5] M. Haescher, D. J. Matthies, J. Trimpop, and B. Urban, "Seismotracker: upgrade any smart wearable to enable a sensing of heart rate, respiration rate, and microvibrations," in *Proceedings of the 2016 CHI Conference Extended Abstracts on Human Factors in Computing Systems*. ACM, 2016, pp. 2209–2216.

[6] F. Attal, S. Mohammed, M. Dedabrishvili, F. Chamroukhi, L. Oukhellou, and Y. Amirat, "Physical human activity recognition using wearable sensors," *Sensors*, vol. 15, no. 12, pp. 31 314–31 338, 2015.

[7] D. J. Matthies, B. A. Strecker, and B. Urban, "Earfieldsensing: a novel in-ear electric field sensing to enrich wearable gesture input through facial expressions," in *Proceedings of the 2017 CHI Conference on Human Factors in Computing Systems*. ACM, 2017, pp. 1911–1922.

[8] A. Alahi, A. Haque, and L. Fei-Fei, "Rgb-w: When vision meets wireless," in *2015 IEEE International Conference on Computer Vision (ICCV)*, no. EPFL-CONF-230282. IEEE, 2015, pp. 3289–3297.

[9] N. Xiao, P. Yang, Y. Yan, H. Zhou, and X.-Y. Li, "Motion-fi: Recognizing and counting repetitive motions with passive wireless backscattering," in *IEEE INFOCOM 2018-IEEE Conference on Computer Communications*. IEEE, 2018, pp. 2024–2032.

[10] J. Huang, B. Liu, H. Jin, and Z. Liu, "Wianti: An anti-interference activity recognition system based on wifi csi," in *2018 IEEE International Conference on Internet of Things (iThings) and IEEE Green Computing and Communications (GreenCom) and IEEE Cyber, Physical and Social Computing (CPSCom) and IEEE Smart Data (SmartData)*. IEEE, 2018, pp. 58–65.

[11] M. Kotaru, K. Joshi, D. Bharadia, and S. Katti, "Spotfi: Decimeter level localization using wifi," in *ACM SIGCOMM Computer Communication Review*, vol. 45, no. 4. ACM, 2015, pp. 269–282.

[12] D. Vasisht, S. Kumar, and D. Katabi, "Decimeter-level localization with a single wifi access point." in *NSDI*, 2016, pp. 165–178.

[13] Y. Wang, K. Wu, and L. M. Ni, "Wifall: Device-free fall detection by wireless networks," *IEEE Transactions on Mobile Computing*, vol. 16, no. 2, pp. 581–594, 2017.

[14] Q. Xu, Y. Chen, B. Wang, and K. R. Liu, "Trieds: Wireless events detection through the wall," *IEEE Internet of Things Journal*, vol. 4, no. 3, pp. 723–735, 2017.

[15] J. Huang, B. Liu, P. Liu, C. Chen, N. Xiao, Y. Wu, C. Zhang, and N. Yu, "Towards anti-interference wifi-based activity recognition system using interference-independent phase component," in *IEEE INFOCOM 2020-IEEE Conference on Computer Communications*. IEEE, 2020, pp. 576–585.

[16] K. Ali, A. X. Liu, W. Wang, and M. Shahzad, "Recognizing keystrokes using wifi devices," *IEEE Journal on Selected Areas in Communications*, vol. 35, no. 5, pp. 1175–1190, 2017.

[17] J. Huang, B. Liu, C. Chen, H. Jin, Z. Liu, C. Zhang, and N. Yu, "Towards anti-interference human activity recognition based on wifi subcarrier correlation selection," *IEEE Transactions on Vehicular Technology*, vol. 69, no. 6, pp. 6739–6754, 2020.

[18] N. Yu, W. Wang, A. X. Liu, and L. Kong, "Qgesture: Quantifying gesture distance and direction with wifi signals," *Proceedings of the ACM on Interactive, Mobile, Wearable and Ubiquitous Technologies*, vol. 2, no. 1, p. 51, 2018.

[19] "Ieee standard for information technology," *IEEE Std 802.11n-2009*, pp. 1–565, Oct 2009.

[20] W. Jiang, C. Miao, F. Ma, S. Yao, Y. Wang, Y. Yuan, H. Xue, C. Song, X. Ma, D. Koutsonikolas *et al.*, "Towards environment independent device free human activity recognition," in *Proceedings of the 24th Annual International Conference on Mobile Computing and Networking*, 2018, pp. 289–304.

[21] D. Halperin, W. Hu, A. Sheth, and D. Wetherall, "Tool release: Gathering 802.11 n traces with channel state information," *ACM SIGCOMM Computer Communication Review*, vol. 41, no. 1, pp. 53–53, 2011.

[22] S.-N. Yu and Y.-H. Chen, "Electrocardiogram beat classification based on wavelet transformation and probabilistic neural network," *Pattern Recognition Letters*, vol. 28, no. 10, pp. 1142–1150, 2007.

[23] S. Wold, K. Esbensen, and P. Geladi, "Principal component analysis," *Chemometrics and intelligent laboratory systems*, vol. 2, no. 1-3, pp. 37–52, 1987.

[24] F. Pedregosa, G. Varoquaux, A. Gramfort, V. Michel, B. Thirion, O. Grisel, M. Blondel, P. Prettenhofer, R. Weiss, V. Dubourg *et al.*, "Scikit-learn: Machine learning in python," *Journal of machine learning research*, vol. 12, no. Oct, pp. 2825–2830, 2011.

[25] Y. Liu and S. Liao, "Preventing over-fitting of cross-validation with kernel stability," in *Joint European Conference on Machine Learning and Knowledge Discovery in Databases*. Springer, 2014, pp. 290–305.

[26] C. Han, K. Wu, Y. Wang, and L. M. Ni, "Wifall: Device-free fall detection by wireless networks," in *IEEE INFOCOM*, 2014, pp. 271–279.